LAND DEGRADATION & DEVELOPMENT

Land Degrad. Develop. **18**: 41–54 (2007)

Published online 11 August 2006 in Wiley InterScience (www.interscience.wiley.com). **DOI**: 10.1002/ldr.762

MAPPING AND MONITORING LAND DEGRADATION RISKS IN THE WESTERN BRAZILIAN AMAZON USING MULTITEMPORAL LANDSAT TM/ETM+ IMAGES

D. LU,[1]* M. BATISTELLA,[2] P. MAUSEL[3] E. MORAN[1,4]

[1]*Center for the Study of Institutions, Population, and Environmental Change (CIPEC), Indiana University, Bloomington, Indiana, USA*
[2]*Brazilian Agricultural Research Corporation, EMBRAPA Satellite Monitoring, Campinas, São Paulo, Brazil*
[3]*Department of Geography, Geology, and Anthropology, Indiana State University (ISU), Terre Haute, Indiana, USA*
[4]*Anthropological Center for Training and Research on Global Environmental Change (ACT), Indiana University, Bloomington, Indiana, USA*

Received 28 February 2006; Revised 16 April 2006; Accepted 2 May 2006

ABSTRACT

Mapping and monitoring land degradation in areas under human-induced stresses have become urgent tasks in remote sensing whose importance has not yet been fully appreciated. In this study, a surface cover index (SCI) is developed to evaluate and map potential land degradation risks associated with deforestation and accompanying soil erosion in a Western Brazilian Amazon rural settlement study area. The relationships between land-use and land-cover (LULC) types and land degradation risks as well as the impacts of LULC change on land degradation are examined. This research indicates that remotely sensed data can be effectively used for identification and mapping of land degradation risks and monitoring of land degradation changes in the study area. Sites covered by mature forest and advanced successional forests have low land degradation risk potential, while some types of initial successional forests, agroforestry/perennial agriculture and pasture have higher risk potential. Deforestation and associated soil erosion are major causes leading to land degradation, while vegetation regrowth reduces such problems. Copyright © 2006 John Wiley & Sons, Ltd.

KEY WORDS: land degradation risk; surface cover index; spectral mixture analysis; Landsat TM/ETM+; Amazon; Brazil

INTRODUCTION

Land degradation has long been recognised as a critical ecological and economic issue due to its impacts on food security and environmental conditions. It involves physical, chemical and biological processes. Physical processes include alterations in soil structure, environmental pollution and unsustainable use of natural resources; chemical processes include acidification, leaching, salinisation, decrease in cation retention capacity and fertility depletion and biological processes include reduction of biomass and biodiversity (Eswaran *et al.*, 2001). In general, land degradation is a slow, almost imperceptible, process that is often neglected or goes unnoticed by the local population, at least during its initial stage. However, when land is in a state of advanced degradation, restoration becomes difficult and/or requires a considerable investment for mitigation. The causes of land degradation are diverse and reflect complex interactions. Different regions may have significantly different drivers of land degradation, including biophysical, socioeconomic and political factors. Natural hazards, population change, marginalisation, poverty, land ownership problems, political instability and maladministration, economic and social issues, health problems and inappropriate land use are among some factors cited in the literature (Barrow, 1991, Johnson and Lewis, 1995). Barrow (1991) summarised the reasons

* Correspondence to: D. Lu, School of Forestry and Wildlife Sciences, Auburn University, 602 Duncan Drive, Auburn, AL 36849, USA.
E-mail: DZL0001@auburn.edu

Contract/grant sponsor: National Science Foundation; contract/grant number: 99-06826.
Contract/grant sponsor: National Aeronautics and Space Administration; contract/grant number: NCC5-695.
Contract/grant sponsor: Embrapa Satellite Monitoring.

causing land degradation in different environments, such as rainforests, seasonally dry tropical, Mediterranean, temperate, wetlands, tundra, islands and dry lands.

Different definitions of land degradation are used in previous literature. For example, FAO (1980) defines land degradation as deterioration or total loss of the productive capacity of the soils for present or future use. Barrow (1991) defines it as the loss of utility or potential utility or the reduction, loss or change of features or organisms that cannot be replaced. Eswaran *et al.* (2001) defines it as the loss of actual or potential productivity or utility as a result of natural or anthropic factors; that is, the decline in land quality or reduction in its productivity. Different regions may present different forms of land degradation, such as depletion of soil nutrients, salinisation, agrochemical pollution, soil erosion and biodiversity loss (Scherr and Yadav, 2001). This makes the evaluation of land degradation a difficult task because of the lack of effective methods and suitable criteria to quantitatively analyse the process.

The criteria for assessing land degradation may be physical/biological (e.g. reduced genetic diversity, species extinction, soil erosion and pollution) and socioeconomic (e.g. farm productivity decline, increased water treatment cost, lack of infrastructure and labour scarcity) (Wasson, 1987). In practise, different indicators, such as soil erosion and soil fertility decline, salinisation and loss of vegetation cover, are often used to assess the status of land degradation. Stocking and Murnaghan (2001) provided many indicators of soil loss and of production constraints and combined indicators for the evaluation of land degradation.

Different methods have been used for land degradation studies, including field observation and evaluation, expert judgement (Sonneveld, 2003) and use of remote sensing and GIS approaches (Amissah-Arthur *et al.*, 2000, Sujatha *et al.*, 2000, Haboudane *et al.*, 2002, Thiam, 2003, Wessels *et al.*, 2004). Remote sensing techniques provide important tools for generating information on land degradation status and its geographical extent (Eiumnoh, 2001, Symeonakis and Drake, 2004, Wessels *et al.*, 2004). For example, Amissah-Arthur *et al.* (2000) used SPOT data, combined with biophysical (e.g. soil quality) and socioeconomic data (e.g. land use intensity, population density and carrying capacity and agricultural intensification) to assess land degradation status in African Sahel. Sujatha *et al.* (2000) used Landsat MSS and TM data to map and monitor degraded lands caused by water logging and subsequent salinisation /alkalinisation in Uttar Pradesh, India, based on visual interpretation of multitemporal images. Haboudane *et al.* (2002) used indices describing the spectral response and behaviour to map the spatial distribution of regional patterns of land degradation in Guadalentin basin in southeastern Spain. Almeida-Filho and Shimabukuro (2002) used multitemporal TM data to map and monitor evolution of degraded areas caused by independent gold miners, based on images segmentation/region classification techniques and post-classification comparison, in the Roraima State, Brazilian Amazon. Thiam (2003) used AVHRR NDVI image in combination with rainfall, soil types, human impact areas and field survey data to assess the risk of land degradation in southern Mauritania.

Most previous research on land degradation was conducted in semiarid or arid environments (Hoffman and Todd, 2000, Taddese, 2001, Symeonakis and Drake, 2004). A combination of remotely sensed classification results and associated ancillary data is often used to map land degradation, but marginal classification results and availability of high-quality ancillary data often reduces its success. In the Brazilian Amazon, policies encouraging large-scale development projects and land conversion are major factors contributing to deforestation (Barbier, 1997), leading to changes in soil structure, loss of soil fertility and soil erosion. Mapping and monitoring land degradation has become an urgent task in this region, but such studies have not attracted sufficient attention yet. Land degradation in the Amazon basin is mainly caused by deforestation and associated soil erosion; thus, a key to exploring land degradation risk relationships requires good land-use and land-cover (LULC) types and an understanding of relationships between LULC and land degradation risks. Hence, this paper explores an approach based on the Surface Cover Index (SCI) to quickly evaluate and map land degradation risks.

STUDY AREA

The study area, located in northeastern Rondônia, is approximately 1600 km^2 (36·5 × 44·0 km) (Figure 1). Settlement began in the early-1980s and deforestation occurred as a result of land use and occupation. Colonists

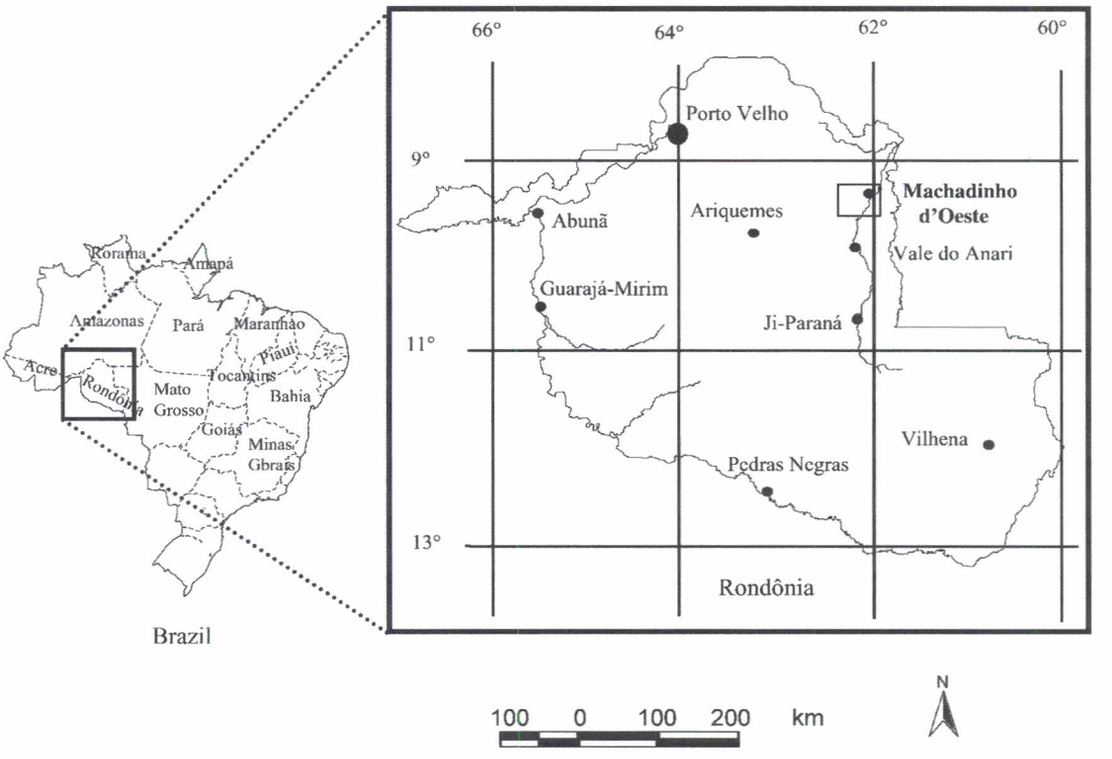

Figure 1. Location of Machadinho d'Oeste in the State of Rondônia, Brazil.

have transformed the forested landscape into a mosaic of cultivated crops, pastures and different stages of secondary succession and forest remnants. The terrain is undulating, ranging from 100 to 350 m above sea level. Several soil types, such as alfisols, oxisols, ultisols and alluvial soil orders, have been identified (Bognola and Soares, 1999). A well-defined dry season lasts from June to August. The annual average precipitation is 2016 mm, and the annual average temperature is 25·5°C (Rondônia, 1998).

METHODS

Figure 2 illustrates the framework for mapping and monitoring land degradation risks using multitemporal Landsat TM/ETM+ images. The major steps include (1) image preprocessing, including geometric rectification, image registration and atmospheric correction; (2) LULC classification using a maximum likelihood classifier (MLC); (3) LULC change detection using a post-classification comparison approach; (4) development of fraction images using the spectral mixture analysis (SMA) approach; (5) mapping of land degradation risks based on a SCI; (6) monitoring of land degradation trends; (7) examination of relationships between land degradation risks and LULC types and (8) examination of interactions between LULC change and land degradation trends.

Data Collection and Preprocessing

Fieldwork was conducted during the dry seasons of 1999, 2000, 2002 and 2003. Preliminary image classification and band composite printouts were used to identify candidate areas to be surveyed, and a flight over the areas provided visual insights about the size, condition and accessibility of each site. The surveys were conducted in areas with relatively homogeneous ecological conditions (e.g. topography, distance from water and land use) and uniform physiognomic characteristics. Secondary succession, mature forest, pasture and agroforestry/perennial agriculture

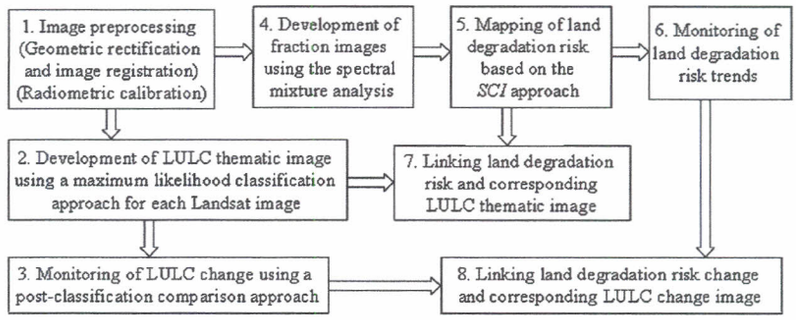

Figure 2. Framework for mapping and monitoring land degradation risks.

plots were identified during fieldwork. Every plot was registered using a global positioning system (GPS) to allow integration with other spatial data in geographic information systems (GIS) and image processing systems. A detailed description of field data collection is provided in Lu *et al.* (2004a). Field data were separated into two groups, one for training samples used in the maximum likelihood classification, and another for test samples for classification accuracy assessment of the 1998 TM and 2002 ETM+ images.

Four dates of Landsat TM/ETM+ data were used in this study. Landsat 5 TM data that were acquired on 18 June 1998, were first geometrically rectified using control points taken from topographic maps at 1:100 000 scale (Universal Transverse Mercator, South 20 zone). The other three dates of images (i.e. 28 July 1988 TM; 15 July 1994 TM and 27 June 2002 ETM+) were registered to the same coordinates as the 1998 TM image. A nearest-neighbour resampling technique was used when implementing geometrical rectification and image registration. A root-mean-square error of less than 0·5 pixels for each registration process was obtained. An improved image-based dark object subtraction model was used to implement radiometric and atmospheric correction (Chavez, 1996, Lu *et al.*, 2002). The surface reflectance values after calibration ranged from 0 to 1. For the convenience of data analysis, the reflectance values were rescaled to the range between 0 and 100 by multiplying the value of 100 to each post-calibration pixel.

Image Classification and Change Detection

Before implementing classification for the 2002 ETM+ data, training sample plots were selected based on field data collected in 2002. LULC classes included mature forest, secondary succession, agroforestry/perennial agriculture, pasture, infrastructure and water. For each class, 15 to 20 training samples were selected and then a maximum likelihood classifier (MLC) was used to classify the 2002 ETM+ data into a thematic map. A similar procedure was used to classify the other three dates of TM images. The samples used to classify the 1998 TM image were collected in 1999 and 2000, that is, a majority of successional forests, agroforestry/perennial agriculture and pasture sample plots were collected during the fieldwork in 1999, and more sample plots of other different land cover classes were collected during fieldwork conducted in 2000. Because of the similar spectral signatures found for agroforestry and secondary succession stages, visual interpretation of TM/ETM+ is often not suitable to identify these classes, thereby harming the collection of sufficient training sample data for the 1994 and 1988 image classifications. For the purposes of this study, agroforestry and successional forests are combined as a single class, SS_AgF, out of necessity, realising that their separation is desirable whenever possible. However, based on field data in the study area, it is evident that similar vegetation stand structure and density between agroforestry and successional forests exist that have similar function in protecting land from degradation. Moreover, most of the agroforestry sites include vegetation in some stage of succession. Local land owners believe that using particular successional species such as *Cecropia* sp. for shading is a good practise for their agroforestry systems. Therefore, the training samples for mature forest, SS_AgF, pasture, infrastructure and water were mainly collected based on visual interpretation of colour composites for 1994 and 1988 TM image classifications. Interviews with local land owners were conducted to understand land use history and to check the accuracy of the selected training samples. After classification, a

majority filter with 3 × 3 window size was used to remove the "salt and pepper" effect on the classified images. A detailed description of MLC approach for LULC classification in the study area is found in Lu *et al.* (2004a).

Accuracy assessment is required for evaluating the classification results. A common method is through the use of an error matrix. Many parameters, such as overall accuracy, producer's accuracy, user's accuracy and Kappa coefficient, can be derived from the error matrix. Previous literature has detailed the accuracy assessment procedures (Congalton *et al.*, 1983, Congalton, 1991, Smits *et al.*, 1999, Foody, 2002). In this paper, accuracy assessment was implemented for the 1998 and 2002 classified images using an IKONOS image acquired on 28 May 2001 and field data collected in 2000 and 2003, respectively. A total of 320 test sample plots were selected for 1998 and 365 test sample plots for 2002. However, no accuracy assessment was performed for 1988 and 1994 because of the difficulty in collecting sufficient reference data.

Although many change detection approaches have been developed (Singh, 1989, Lu *et al.*, 2004b), the post-classification comparison approach is still often used for detecting LULC trajectories. Such approach was also used in this research. Four classes (i.e. forest, SS_AgF, pasture and non-vegetation) were used in the vegetation change detection analysis and land degradation analysis. Five change trajectories were identified, that is, (1) from mature forest to SS_AgF, (2) from mature forest to pasture, (3) from SS_AgF to pasture, (4) from pasture to SS_AgF and (5) other changes such as the conversion of different LULC classes to infrastructure or to water. Three change detection images were generated based on a pixel-by-pixel comparison approach of two classified images between 1988 and 1994, between 1994 and 1998 and between 1998 and 2002, respectively. The accuracy assessment for the 1998–2002 change detection result was conducted based on field data collected in 2000 and 2003, respectively. Accuracy assessments for the remaining two change detection periods were not implemented because of the difficulty in collecting time-series reference data.

Development of Fraction Images

Spectral mixture analysis (SMA) is regarded as a physically based image processing tool. It supports repeatable and accurate extraction of quantitative subpixel information (Smith *et al.*, 1990). The SMA approach assumes that the spectrum measured by a sensor is a linear combination of the spectra of all components (endmembers) within the pixel and the spectral proportions of the endmembers reflect proportions of the area covered by distinct features on the ground (Adams *et al.*, 1995). The mathematic model of SMA can be expressed as

$$R_i = \sum_{k=1}^{n} f_k R_{ik} + \varepsilon_i \tag{1}$$

where $i = 1, \ldots, m$ (number of spectral bands); $k = 1, \ldots, n$ (number of endmembers); R_i is the spectral reflectance of band i of a pixel, which contains one or more endmembers; f_k is the proportion of endmember k within the pixel; R_{ik} is known as the spectral reflectance of endmember k within the pixel on band i, and ε_i is the error for band i. For a constrained unmixing solution, f_k is subject to the following restrictions:

$$\sum_{k=1}^{n} f_k = 1 \text{ and } 0 \leq f_k \leq 1 \tag{2}$$

The root mean square error (RMSE) is often used to assess the fit of the model. The RMSE is computed based on errors and number of spectral bands used, that is,

$$\text{RMSE} = \sqrt{\left(\sum_{i=1}^{m} \varepsilon_i^2\right) \Big/ m} \tag{3}$$

In the SMA approach, selecting sufficiently high-quality endmembers is a key for successfully developing high-quality fraction images. Many factors, such as the purpose of the study, image data used, the scale and complexity

of landscape in the study area and the analyst's knowledge and skills, can affect the selection of endmembers. Many methods for endmember selection have been developed (Smith *et al.*, 1990, Settle and Drake, 1993, Bateson and Curtiss, 1996, Tompkins *et al.*, 1997, Mustard and Sunshine, 1999, van der Meer, 1999, Dennison and Roberts, 2003, Theseira *et al.*, 2003), but the image-based endmember selection approach is preferred because endmembers can be easily obtained and they represent the spectra measured at the same scale as the image data. In general, image endmembers are derived from the extremes of the image feature space, assuming they represent the purest pixels in the images (Mustard and Sunshine, 1999, Lu *et al.*, 2003). In this study, three endmembers (i.e. green vegetation, shade and soil) were selected based on the scatterplots of TM/ETM+ bands 3 and 4 and TM/ETM+ bands 4 and 5. After determination of endmembers, a constrained least-squares solution was used to unmix the multispectral images into three endmember fraction images. The same method was used to unmix each date of multispectral TM/ETM+ images into shade, green vegetation and soil fraction images, respectively.

Mapping and Monitoring Land Degradation Risks

The factors affecting land degradation often vary depending on the characteristics of specific study areas because different regions may have significantly different causes inducing land degradation. In the Brazilian Amazon basin, deforestation associated with high temperature and precipitation is an important factor inducing soil erosion and rapid loss of soil nutrients, resulting in land degradation. In general, vegetation cover and vegetation stand structure are important factors protecting land from degradation. Dense vegetation cover associated with multiple layers of stand structure can effectively intercept raindrops, minimising their impact on soils and consequent erosion processes. In tropical rainforests, most soils have low fertility; therefore, nutrient cycling is an important mechanism for ecosystem maintenance. High temperature and humidity lead to a rapid turnover of nutrients between vegetation, litter and soil. Severe land degradation problems can occur if vegetation cover is removed or disturbed, because it plays an important role in maintaining soil structure and nutrient cycling (Lavelle, 1987, Moran *et al.*, 2000).

The loss of soil by erosion may be a good indicator for evaluating land degradation in the Brazilian Amazon. However, the estimation of soil erosion losses is often difficult because of interplaying factors, such as topography, ground cover and precipitation. In particular, mapping of soil erosion losses over large areas is a challenging task, requiring a remote sensing-based approach for rapidly mapping the potential risks of land degradation. Land cover features captured by remote sensors provide a powerful insight for land degradation research. It is well known that high vegetation density associated with a complex stand structures can effectively reduce soil loss by erosion. For densely advanced successional forests or mature forest, the soil erosion is very limited, but after deforestation, the uncovered land can result in high soil erosion rates and rapid land degradation. An index representing land cover surface conditions may be useful for rapidly assessing land degradation risks. Such land cover surface information can be developed from remotely sensed data. In this paper, it is assumed that land degradation risk is minimal in advanced successional forests and mature forests. For other vegetation classes, a SCI is designed to evaluate the potential risk of land degradation. The index is defined as:

SCI = 0, when f_{gv} is greater than 70 per cent and f_{shade} is greater than 20 per cent,

$$\text{otherwise, } \text{SCI} = \frac{1}{2}(1 + f_{soil} - f_{gv} - f_{gv} * f_{shade}) * 100 \tag{4}$$

where f_{soil}, f_{gv} and f_{shade} are the proportions of soil, green vegetation and shade in a unit, respectively. They meet the following conditions: $f_{soil} + f_{gv} + f_{shade} = 1$ and all of them range from 0 and 1. The SCI ranges from 0 to 100. When the site is covered with dense vegetation, such as dense pasture or grass, f_{gv} is close to 1 and f_{soil} and f_{shade} are close to 0, then SCI is close to 0. When the site is covered with no or very little vegetation, f_{soil} is close to 1, f_{gv} and f_{shade} is close to 0, then SCI is as high as 100. Higher SCI values indicate higher potential risk of land degradation. The variables used in the SCI equation are derived from the Landsat TM/ETM+ data based on the SMA approach.

Linking Land Degradation Risks to LULC Data

The SCI was calculated based on fraction images for each analysed date. The SCI values for typical LULC classes, such as mature forest, initial (SS1), intermediate (SS2) and advanced (SS3) successional forests, coffee plantation and pasture, were analysed in 2002 and 1998 SCI images. A detailed description of stand structure among the successional forest stages is found in Lu *et al.* (2003). The analysis of SCI values for the typical land cover classes indicates that the majority of mature forest and SS3 have SCI values of less than 30; the majority of SS1, SS2 and coffee plantation have SCI values between 30 and 50; and most pasture and some SS1 areas have SCI values greater than 50. Therefore, three levels of land degradation risks, that is, low, medium and high, were defined when SCI value falls between 0–30, 30–50 and 50–100, respectively. A SCI ranked image was generated for each date based on such thresholds. The ranked SCI images and corresponding LULC classification images were then integrated in a GIS. They were compared on a pixel-by-pixel basis, generating the statistical results that demonstrate the relationships between land degradation risks and LULC types.

Before analysing the change of land degradation risks, that is, increasing or decreasing risks, it is required to give a definition of the change trajectories of land degradation risks. If a site with low degradation risk at a prior date is changed to medium or high risk at a later date, this site is defined as increasing degradation risk. In contrast, if a site with high or medium degradation risk at a prior date is changed to medium or low risk at a later date, this site is defined as decreasing degradation risk. Thus, the spatial distribution of increasing or decreasing risks can be illustrated in an image through implementing the comparison of two ranked SCI images. In order to examine how different LULC changes affect land degradation risk trends, a pixel-by-pixel comparison of LULC change image and the corresponding SCI change image for the same period is conducted and the statistical results are produced for analysing the impacts of LULC changes on land degradation risks.

Validation of the Land Degradation Risk Maps

Validation of a model is an important aspect of evaluating its performance. The determination of thresholds used for classifying land degradation risk levels greatly depends on availability of ground reference data. Because of the lack of reference data, quantitative validation of the land degradation risk results was not implemented in this study. However, visual interpretation of the land degradation risk maps was conducted by an expert who had worked in the study area for many years. This article's primary focus is to develop a theoretical approach to rank land degradation risks using elements of spectral mixing theory that emphasises the land components of green vegetation, soil/bare and shade/shadow in an Amazonian environment. Although informative, this research can be considered as preliminary. Further studies are needed in search of more advanced and universal models based on the integration of remotely sensed and ground reference data.

RESULTS

Image Classification and Change Detection Results

Figure 3 illustrates the classification results for the analysed dates. A comparison between these images indicates that the area covered by mature forest was significantly reduced from 1988 to 1994, and until 2002. However, different stages of successional forests, agroforestry and pastures occupied the deforested areas. Accuracy assessment indicates that overall accuracies of greater than 91 per cent are achieved for the 1998 TM and 2002 ETM+ image classifications including five LULC classes. Although the accuracies for the 1994 and 1988 TM image classifications are not known, visual comparison of the classification image with corresponding TM colour composite and responses from interviews with local land owners indicate that the classifications are satisfactory for the purposes of this study. The results for LULC classifications are summarised in Table I. The value for each LULC class represents its percentage accounted for the study area. In this study, the total area is 1602·21 km^2. The mature forest decreases approximately 37 per cent for the period analysed, from 88 per cent in 1988 to 51 per cent in 2002. The SS_AgF increases approximately 32 per cent during the same period. Pasture and non-vegetation (infrastructure and water) areas also increase from 1988 to 2002.

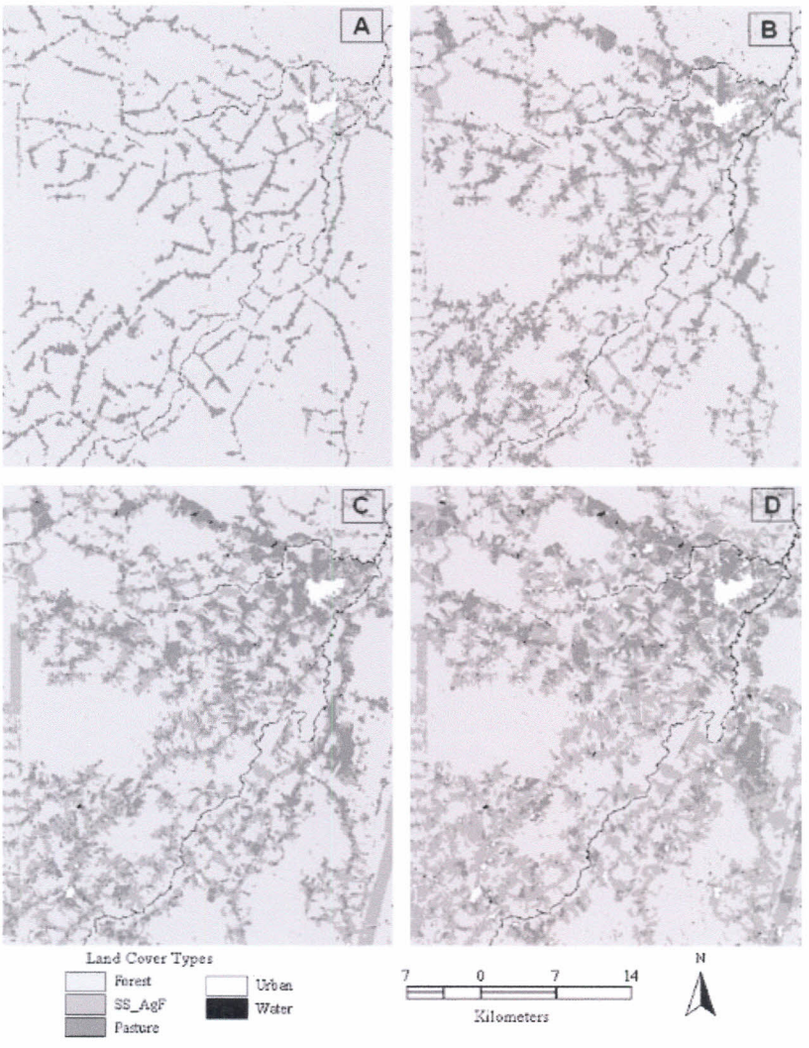

Figure 3. Mapping of land-use and land-cover distributions using Landsat TM/ETM+ images (A: 1988; B: 1994; C: 1998 and D: 2002).

Table I. A summary of percentages of areas for Landsat TM/ETM+ image classification results among different dates

Classes	1988	1994	1998	2002
Forest	87.94	73.79	60.25	51.22
SS_AgF	2.68	13.67	24.88	34.85
Pasture	8.50	11.53	13.77	11.68
Nonvegetation	0.88	1.01	1.10	2.25

Note: SS_AgF includes different successional stages and agroforestry/perennial agriculture; and Nonvegetation includes infrastructure and water classes.

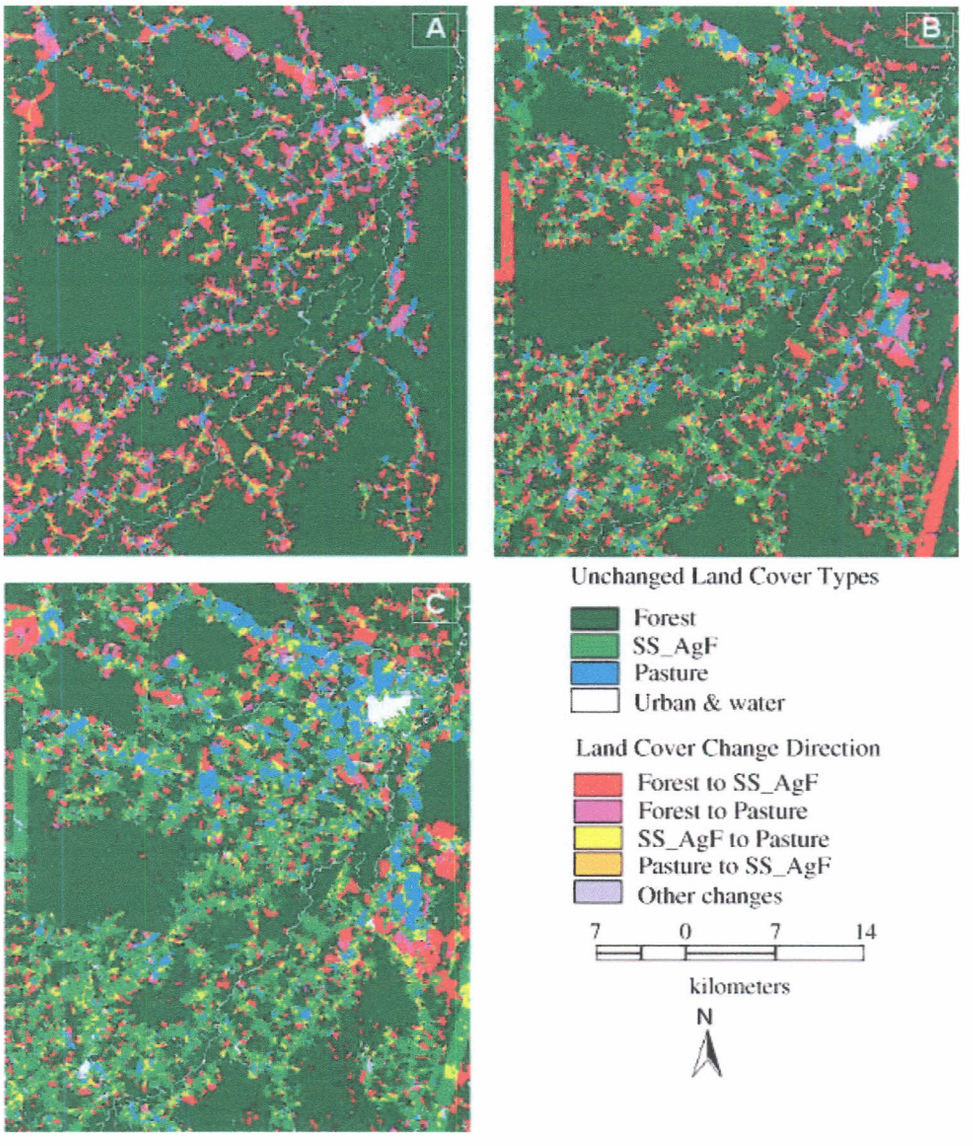

Plate 1. Monitoring of land-use and land-cover change using multitemporal Landsat TM/ETM+ images (A: between 1988 and 1994; B: between 1994 and 1998 and C: between 1998 and 2002).

The land cover change detection results are illustrated in Plate 1. Between 1988 and 1994, the major change is due to the conversion of mature forest to SS_AgF and pasture. During the periods of 1994–1998 and 1998–2002, many deforested areas are occupied by different stages of SS_AgF and pasture. The accuracy assessment for the 1998–2002 change detection result indicates that an overall accuracy of approximate 85 per cent for the five change trajectories is obtained. The quantitative land cover changes are summarised in Table II. The average annual deforestation rates (conversion of mature forest to agroforestry or pasture or succession) are 2·34 per cent, 3·55 per cent and 2·7 per cent for the three change detection periods between 1988 and 2002. These deforestation rates are much higher than for the entire Rondonia State or the entire Brazilian Amazon (which ranges from 0·61 per cent to 1·65 per cent, and from 0·3 per cent to 0·54 per cent between 1988 and 2000, respectively except in 1995 when the rate was 2·62 per cent for Rondonia and 0·8 per cent for Amazonia) (Instituto Nacional de Pesquisas Espaciais (INPE, 2002)). The transform rates between SS_AgF and pasture also increase during these change detection periods. For example, the annual change rate from SS_AgF to pasture or from pasture to SS_AgF was 0·84 per cent between 1988 and 1994, 1·79 per cent between 1994 and 1998 and 2·25 per cent between 1998 and 2002. Usually, the most common initial land cover following deforestation is pasture or crops. After a few years, land can be abandoned initiating a fallow cycle. Shrubs and trees gradually dominate until an advanced succession stage is achieved if no disturbance occurred. However, at any successional stage, human activities can interrupt the regeneration process by reintroducing crops, cattle ranching and perennial agriculture or agroforestry.

Analysis of Land Degradation Risk

Figure 4 shows the ranked SCI images for the four analysed dates. An obvious finding from these SCI images is that most of the study area has low potential risk of land degradation. However, the areas with medium and high potential risks of land degradation increased significantly from 1988 to 2002. In 1988, the majority of the study area was covered by mature forest and high-risk areas are mainly located in the deforested areas along the road system. As deforested areas increase, the high-risk patches also increase. This is particularly visible in the 2002 SCI image that implies deforestation is an important factor leading to the land degradation.

An integrative analysis of the SCI images and corresponding LULC classification images for each date reveals relationships between potential risk of land degradation and land cover types. Table III summarises the statistical results of area percentages for each SCI rank level and corresponding LULC types. Non-vegetation (infrastructure and water) was not included because the interest on land degradation risks was focused on forest, successional stages, agricultural lands and pasture lands. Analysis of the results indicated that the area of low risk decreased from approximately 92·1 per cent in 1988 to 73·6 per cent in 2002. Conversely, the area of high risk increased from approximately 4·0 per cent in 1988 to 9·0 per cent in 2002, and the area of medium risk increased from

Table II. A summary of change detection results (percentage of area for each category)

Categories	Change detection periods		
	1988–1994	1994–1998	1998–2002
Unchanged classes			
Forest	74.05	59.91	49.74
SS_AgF	1.30	9.40	19.41
Pasture	4.16	6.78	7.03
Nonvegetation	0.88	0.86	1.19
Change trajectory			
Forest to SS_AgF	8.06	10.76	9.42
Forest to Pasture	6.03	3.46	1.38
SS_AgF to Pasture	1.09	3.15	3.18
Pasture to SS_AgF	3.95	4.01	5.83
Other changes	0.48	1.67	2.82

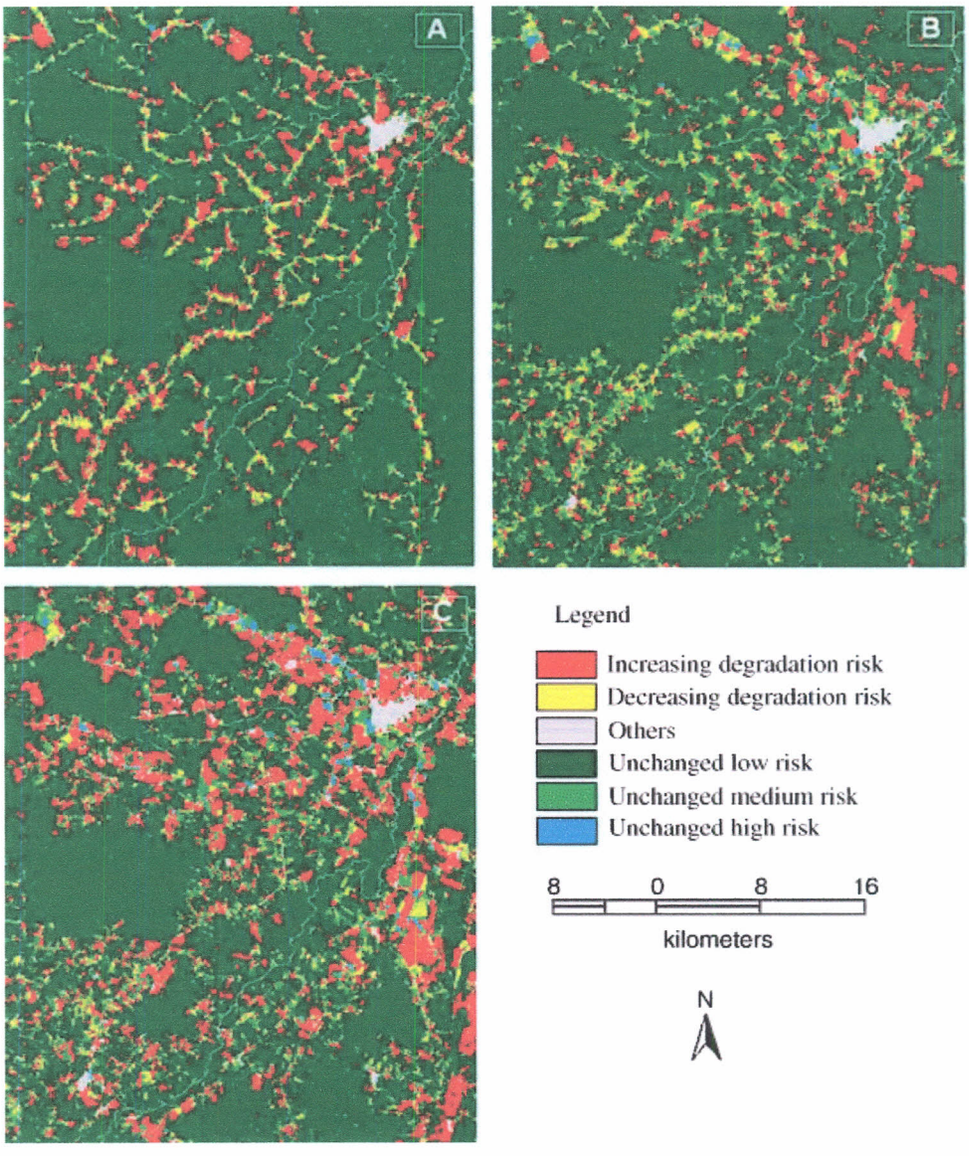

Plate 2. Monitoring of land degradation risk changes using multitemporal Landsat TM/ETM+ images (A: between 1988 and 1994; B: between 1994 and 1998 and C: between 1998 and 2002).

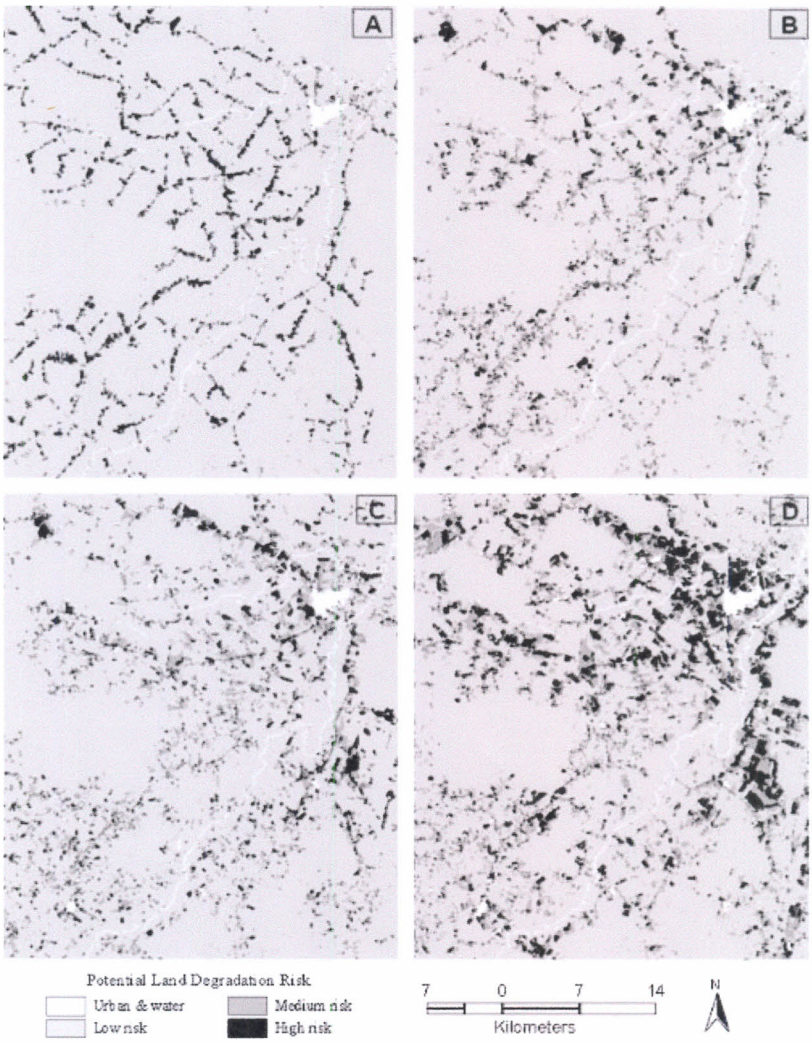

Figure 4. Mapping of land degradation risks using Landsat TM/ETM+ images (A: 1988; B: 1994; C: 1998 and D: 2002).

approximately 2·0 per cent to 13·7 per cent in the same period. Most of pasture and some SS_AgF classes were found in the medium and high land degradation risk categories.

A comparison of ranked SCI images between different dates can be used to demonstrate the spatial distributions of the change in land degradation risks, as illustrated in Plate 2. The areas with increasing degradation risk increase significantly from 1988 until 2002, especially between 1998 and 2002. These results are summarised in Table IV. For unchanged SS_AgF or pasture vegetation during the change detection periods, both increasing and decreasing risks occurred. The short-term rotation periods between successional forests and/or agroforestry, the disturbance or growth in the successional forest stages cause the change of degradation risks. For example, successional forest growth from initial to intermediate successional stages reduces the risk of land degradation, but the human induced disturbance causing the transform of intermediate stage to initial successional stage increases the risk of land degradation. The long term overgrazing on the pasture lands can make the pasture conditions poor, increasing the risks of land degradation. For changed vegetation areas, deforestation (conversion of mature forest in prior date to

Table III. A comparison of land degradation risk areas among vegetation types in different dates (percentages of area)

Year	Classes	Low	Medium	High
1988	Forest	86.92	0.59	0.18
	SS_AgF	2.46	0.11	0.03
	Pasture	2.68	1.34	3.76
	Total	92.06	2.04	3.97
1994	Forest	73.26	0.38	0.03
	SS_AgF	11.62	1.87	0.01
	Pasture	2.36	5.26	3.34
	Total	87.24	7.51	3.38
1998	Forest	59.74	0.33	0.05
	SS_AgF	21.00	2.95	0.32
	Pasture	3.91	4.96	4.31
	Total	84.65	8.24	4.68
2002	Forest	50.90	0.16	0.03
	SS_AgF	22.43	9.91	1.57
	Pasture	0.28	3.60	7.43
	Total	73.61	13.67	9.03

Note: The total percentage was not 100 because urban and water areas were excluded in this study.

pasture, successional forests or agroforestry in a late date) and changes of successional forests or agroforestry to pasture are the main causes of land degradation. The transformation of pasture to successional forests may reduce the degradation risks. Between 1988 and 1994, 7·87 per cent of the study area had increased degradation risks that increased to 8·24 per cent between 1994 and 1998, and grew to 16·52 per cent between 1998 and 2002. Areas with decreasing degradation risks changed from 4·28 per cent to 6·39 per cent during the period of 1988 and 2002. The degradation trend is obviously indicating deterioration as deforestation increased. Table IV also indicates that the conversion from mature forest to SS_AgF or pasture, and from SS_AgF to pasture have a higher possibility to

Table IV. Relationships between land degradation risk change and vegetation change

Period	Category	Risk level	Unchanged classes				Change trajectories			Total
			MF	SS_A	P	MF to SS_A	MF to P	SS_A to P	P to SS_A	
From 1988 to 1994	Unchg risk	Low	73.188	1.064	0.336	6.881	1.114	0.267	0.941	83.791
		Medium	0.043	0.007	0.344	0.036	0.078	0.020	0.100	0.627
		High	0.001	0.000	0.426	0.000	0.012	0.002	0.002	0.443
	Chg risk	Decr. risk	0.271	0.054	1.323	0.181	0.057	0.015	2.379	4.281
		Incr. risk	0.348	0.127	1.186	0.850	4.478	0.719	0.166	7.875
From 1994 to 1998	Unchg risk	Low	59.196	7.191	0.647	8.940	0.549	0.966	0.558	78.047
		Medium	0.017	0.228	1.326	0.017	0.014	0.175	0.421	2.198
		High	0.000	0.000	0.595	0.000	0.001	0.001	0.023	0.620
	Chg risk	Decr. risk	0.200	1.069	2.317	0.104	0.009	0.135	2.558	6.392
		Incr. risk	0.324	0.634	1.383	1.473	2.756	1.734	0.117	8.421
From 1998 to 2002	Unchg risk	Low	49.263	11.983	0.055	5.663	0.042	0.096	0.742	67.845
		Medium	0.010	0.763	0.873	0.050	0.009	0.136	0.855	2.696
		High	0.000	0.014	1.173	0.001	0.002	0.018	0.129	1.337
	Chg risk	Decr. risk	0.158	1.764	0.587	0.098	0.001	0.022	2.646	5.276
		Incr. Risk	0.165	4.002	3.974	3.389	1.275	2.715	0.997	16.517

Note: MF, mature forest; SS_A, successional forests and agroforestry/perennial agriculture; P, pasture; Unchg or Chg risks, unchanged or changed risks; Decr. risk or Incr. risk, decreasing or increasing land degradation risk.
The total percentage in this table was not 100 because urban and water areas were excluded in this study.

induce land degradation, but the change from pasture to SS_AgF can reduce the degradation risks, that is, protecting land from degradation. Conversely, for the unchanged SS_AgF or pasture areas, land can be degraded also because of soil erosion or improper land use.

DISCUSSION AND CONCLUSION

Land degradation assessment is a challenging task and has not obtained sufficient attention in the Amazon basin. The complexity and interplay of drivers causing land degradation vary in different sites, thus there is lack of a suitable approach to implement land degradation assessments. This paper develops a new approach based on purely remote sensing techniques for mapping and monitoring of land degradation risks in a Western Brazilian Amazon study area. It is found that remotely sensed data have the potential to provide new insights for rapidly assessing land degradation risks in large areas. Although detailed assessments of land degradation risk results are not conducted in this paper, visual analyses of the results have indicated that the developed land degradation risk maps appear to be very reasonable and represent the real situation where land cover change increases or decreases land degradation risks. Comparisons between the land degradation risk maps and corresponding land cover classes, or between the land degradation trend images and land cover change trajectories show the promise in use of the SCI approach for evaluating land degradation risk in this study area. The identified relationships between land degradation risks and LULC types and impacts of LULC change on land degradation risks is a first step in providing the foundation for better planning and managing land resources. Understanding these relationships is helpful for better using land resources after deforestation. Some possible applications and implications of this land degradation risk approach may include public policies regarding land management and conservation, land zoning (which has been a major discussion in the Amazon, particularly in Rondônia) and agricultural practises and extension. The approach developed in this paper may describe possible risks from these processes of land occupation and monitor the potential risk trends caused by LULC changes.

Research on land degradation in the Amazon basin has an important role for better management and utility of land resources. This study indicates that deforestation and associated land degradation by soil erosion should be evaluated and monitored. Hence, soil erosion, loss of soil fertility and biomass depletion may be used as indicators for such evaluations. However, the development of these indicators based on field surveys for large areas is not an easy task. Thus, an effective approach to assess this phenomenon is required. The SCI approach developed in this paper is a contribution for mapping and monitoring land degradation risks in the Amazon. In general, land degradation is related to soil conditions, topographic factors and land use history, in addition to the land cover surface characteristics. A combination of SCI and other ancillary data may improve the effectiveness of land degradation evaluation through the development of suitable expert systems or rules. Caution must be taken when the SCI equation is used to other study areas because of their different land cover features and patterns, soil conditions, climates and human activities. Also, remotely sensed data capture the surface features at the time when images are acquired, thus they cannot represent the average status of land degradation within a year. Different seasons may influence the proportions of soil and vegetation in a unit, thus, increasing the temporal resolution of remotely sensed data used in land degradation assessments in order to avoid biases caused by seasonal variations is recommended.

The model used in this paper is only based on three endmembers. For many cases, three endmembers are not sufficient, especially in complex environments. In moist tropical forest areas, vegetation stand structure and species composition are very complex. For an optical satellite sensor such as Landsat TM, the sensor mainly captures information from the leaves, wood and shadowing information for a dense vegetation area. However, for sparse vegetation, soil and litter also can significantly affect reflectance. Not all components selected are resolvable in a given image because of their mixing nature and the degree of spectral contrasts found within pixels. For TM images, high correlations between TM bands limit the number of endmembers to be used in the SMA approach. Also, selecting more than three endmembers is often difficult based on the image-based endmember selection approach. The image endmember method assumes that true endmembers are contained in the data set used, but in practise, this assumption is not always true, depending on the scale and characteristics of the study area. Hence, it is

necessary to use reference endmembers to link image endmembers to actual target materials. A combination of image and reference endmember selection methods, including a spectral alignment of the image endmembers to the reference endmember spectra, and a calibration relating the image endmembers to the reference endmembers has been used to identify four endmembers, including vegetation, shade, non-photosynthetic vegetation (NPV) and soil in the Amazon land cover classification (Adams *et al.*, 1995, Roberts *et al.*, 1998). The inclusion of NPV may improve the quality of fraction images, especially the soil fraction image because the NPV component is often contained in the soil fraction image if NPV endmember is not used in the SMA approach (Roberts *et al.*, 1998). Hence, in the SCI equation, the SCI value may be overestimated because of the influences of NPV factor.

ACKNOWLEDGEMENTS

This project is part of the Large-Scale Biosphere Atmosphere Experiment in Amazônia (LBA) Program, LC-09, which aims to examine the human and physical dimensions of LULC change.

REFERENCES

Adams JB, Sabol DE, Kapos V, Filho RA, Roberts DA, Smith MO, Gillespie AR. 1995. Classification of multispectral images based on fractions of endmembers: Application to land-cover change in the Brazilian Amazon. *Remote Sensing of Environment* **52**: 137–154.

Almeida-Filho R, Shimabukuro YE. 2002. Digital processing of a Landsat-TM time series for mapping and monitoring degraded areas caused by independent gold miners, Roraima State, Brazilian Amazon. *Remote Sensing of Environment* **79**: 42–50.

Amissah-Arthur A, Mougenot B, Loireau M. 2000. Assessing farmland dynamics and land degradation on Sahelian landscapes using remotely sensed and socioeconomic data. *International Journal of Geographical Information Science* **14**: 583–599.

Barbier EB. 1997. The economic determinants of land degradation in developing countries. *Philosophical Transactions Royal Society B* **352**: 891–899.

Barrow CJ. 1991. *Land Degradation: Development and Breakdown of Terrestrial Environments*. Cambridge University Press: Cambridge; 295 p.

Bateson A, Curtiss B. 1996. A method for manual endmember selection and spectral unmixing. *Remote Sensing of Environment* **55**: 229–243.

Bognola IA, Soares AF. 1999. *Solos das 'glebas 01, 02, 03 e 06' do MunicÚpio de Machadinho d'Oeste, RO. Pesquisa em Andamento, n.10*. EMBRAPA Monitoramento por Satélite: Campinas, Brazil; 7 p.

Chavez PS, Jr. 1996. Image-based atmospheric corrections—revisited and improved. *Photogrammetric Engineering and Remote Sensing* **62**: 1025–1036.

Congalton RG. 1991. A review of assessing the accuracy of classification of remotely sensed data. *Remote Sensing of Environment* **37**: 35–46.

Congalton RG, Oderwald RG, Mead RA. 1983. Assessing Landsat classification accuracy using discrete multivariate analysis statistical techniques. *Photogrammetric Engineering and Remote Sensing* **49**: 1671–1678.

Dennison PE, Roberts DA. 2003. Endmember selection for multiple endmember spectral mixture analysis using endmember average RMSE. *Remote Sensing of Environment* **87**: 123–135.

Eiumnoh A. 2001. Tools for identification, assessment, and monitoring of land degradation. In *Response to Land Degradation*, Bridges EM, Hannam ID, Oldeman LR, Penning de Vries FWT, Scherr SJ, Sombatpanit S (eds). Science Publishers, Inc: Enfield, NH, pp. 249–260.

Eswaran H, Lal R, Reich PF. 2001. Land degradation: An overview. In *Response to Land Degradation*, Bridges EM, Hannam ID, Oldeman LR, Penning de Vries FWT, Scherr SJ, Sombatpanit S (eds). Science Publishers, Inc: Enfield, New Hampshire, USA; pp. 20–35.

FAO. 1980. *Natural Resources and the Human Environment for Food and Agriculture*. Environment Paper No. 1. Rome.

Foody GM. 2002. Status of land cover classification accuracy assessment. *Remote Sensing of Environment* **80**: 185–201.

Haboudane D, Bonn F, Royer A, Sommer S, Mehl W. 2002. Land degradation and erosion risk mapping by fusion of spectrally-based information and digital geomorphometric attributes. *International Journal of Remote Sensing* **23**: 3795–3820.

Hoffman MT, Todd S. 2000. A National Review of Land Degradation in South Africa: The influence of Biophysical and Socio-economic Factors. *Journal of Southern African Studies* **26**: 743–758.

Instituto Nacional de Pesquisas Espaciais (INPE). 2002. *Monitoring of the Brazilian Amazon Forest by Satellite 2000-2001*, INPE, São José dos Campos, SP, Brazil; 23 p.

Johnson DL, Lewis LA. 1995. *Land degradation: Creation and Destruction*. Blackwell Publishers: Oxford; 335 p.

Lavelle P. 1987. Biological processes and productivity of soils in the humid tropics. In *The Geophysiology of Amazonia: Vegetation and Climate Interactions*, Robert ED (ed.). Wiley: New York; pp. 175–222.

Lu D, Mausel P, Brondízio E, Moran E. 2002, Assessment of atmospheric correction methods for Landsat TM data applicable to Amazon basin LBA research. *International Journal of Remote Sensing* **23**: 2651–2671.

Lu D, Moran E, Batistella M. 2003. Linear mixture model applied to Amazônian vegetation classification. *Remote Sensing of Environment* **87**: 456–469.

Lu D, Mausel P, Batistella M, Moran E. 2004a. Comparison of land-cover classification methods in the Brazilian Amazon basin. *Photogrammetric Engineering and Remote Sensing* **70**: 723–731.

Lu D, Mausel P, Brondizio E, Moran E. 2004b. Change detection techniques. International *Journal of Remote Sensing* **25**: 2365–2407.

Moran E, Brondízio E, Tucker JM, Da Silva-Forsberg MC, McCracken SD, Falesi I. 2000. Effects of soil fertility and land use on forest succession in Amazônia. *Forest Ecology and Management* **139**: 93–108.

Mustard JF, Sunshine JM. 1999. Spectral analysis for earth science: Investigations using remote sensing data. In *Remote Sensing for the Earth Sciences: Manual of Remote Sensing* (3rd edn, **vol. 3**). Rencz AN (ed.). John Wiley & Sons: NY; pp. 251–307.

Roberts DA, Batista GT, Pereira JLG, Waller EK, Nelson BW. 1998. Change identification using multitemporal spectral mixture analysis: Applications in eastern Amazônia. In *Remote Sensing Change Detection: Environmental Monitoring Methods and Applications*, Lunetta RS, Elvidge CD (eds). Ann Arbor Press: Ann Arbor, MI; pp. 137–161.

Rondônia. 1998. *Diagnœstico Sœcio-Ecoɳmico do Estado de Ronɗnia e Assistõncia TÕcnica para FormulaÓÐo da Segunda AproximaÓÐo do Zoneamento Sœcio-Ecoɳmico-Ecolœgico—Climatologia*, v.1. Governo de Rondônia/PLANAFLORO, Porto Velho, Brasil.

Scherr SJ, Yadav S. 2001. Land degradation in the developing world: issues and policy options for 2020 (chapter 21). In *The Unfinished Agenda: Perspectives on Overcoming Hunger, Poverty and Environmental Degradation*, Pinstrup–Andersen P, Lorch RJ (eds). International Food Policy Research Institute: Washington, DC; pp. 133–138.

Settle JJ, Drake NA. 1993. Linear mixing and the estimation of ground cover proportions. *International Journal of Remote Sensing* **14**: 1159–1177.

Singh A. 1989. Digital change detection techniques using remotely sensed data. *International Journal of Remote Sensing* **10**: 989–1003.

Smith MO, Ustin SL, Adams JB, Gillespie AR. 1990. Vegetation in Deserts: I. A regional measure of abundance from multispectral images. *Remote Sensing of Environment* **31**: 1–26.

Smits PC, Dellepiane SG, Schowengerdt RA. 1999. Quality assessment of image classification algorithms for land-cover mapping: A review and a proposal for a cost-based approach. *International Journal of Remote Sensing* **20**: 1461–1486.

Sonneveld BDJS. 2003. Formalizing expert judgements in land degradation assessment: A case study for Ethiopia. *Land Degradation & Development* **14**: 347–361.

Stocking M, Murnaghan N. 2001. *Handbook for the Field Assessment of Land Degradation*. Earhscan Publications Ltd: London, UK; 169p.

Sujatha G, Dwivedi RS, Sreenivas K, Venkataratnam L. 2000. Mapping and monitoring of degraded lands in part of Jaunpur district of Uttar Pradesh using temporal spaceborne multispectral data. *International Journal of Remote Sensing* **21**: 519–531.

Symeonakis E, Drake N. 2004. Monitoring desertification and land degradation over sub-Saharan Africa. *International Journal of Remote Sensing* **25**: 573–592.

Taddese G. 2001. Land degradation: A challenge to Ethiopia. *Environmental Management* **27**: 815–824.

Theseira MA, Thomas G, Taylor JC, Gemmell F, Varjo J. 2003. Sensitivity of mixture modeling to endmember selection. *International Journal of Remote Sensing* **24**: 1559–1575.

Thiam AK. 2003. The causes and spatial pattern of land degradation risk in southern Mauritania using multitemporal AVHRR-NDVI imagery and field data. *Land Degradation & Development* **14**: 133–142.

Tompkins S, Mustard JF, Pieters CM, Forsyth DW. 1997. Optimization of endmembers for spectral mixture analysis. *Remote Sensing of Environment* **59**: 472–489.

Van der Meer F. 1999. Iterative spectral unmixing (ISU). *International Journal of Remote Sensing* **20**: 3431–3436.

Wasson R. 1987. Detection and measurement of land degradation processes. In *Land Degradation: Problems and Policies*, Chisholm A, Dumsday R (eds). Cambridge University Press; Cambridge; pp. 49–75.

Wessels KJ, Prince SD, Frost PE, van Zyl D. 2004. Assessing the effects of human induced land degradation in the former homelands of northern South Africa with a 1 km AVHRR NDVI time-series. *Remote Sensing of Environment* **91**: 47–67.

